POLITECNICO
MILANO 1863

AIM-7M Sparrow: Conceptual design for upgrades in Range, Velocity and Maneuverability

Filippo Carfagna

Elisa Castoldi

Mattia Dotti

Francesco Gigante

Tommaso Messa

Alessandro Turano

Final Report of Launch Systems

Laboratorio di Propulsione Aerospaziale
Dip. Scienze e Tecnologie Aerospaziali

Academic Year 2017-2018

Abstract

This report explains the procedure to achieve a 20 % increment in range and maximum speed, maintaining a comparable maneuverability with respect to the air-to-air missile selected as a baseline. Throughout the conceptual design, all the main aspects of the missile (aerodynamics, structure and propulsive system) are considered. Starting from a sensitivity analysis regarding the engineering parameters that most affect the performance requirements, different possible improvements have been considered and studied. A way to meet all the requirements at the same time without upsetting too much the existing baseline has not been found.
The proposed solution, featuring a more compact guidance and control system, an elongation of the nose and an upgrade in the rocket motor, enables a 22.62% increase in range and a 10.90% in the maximum speed.
More radical changes with respect to the baseline thats may lead to the desired improvements are suggested at the end of the report.

Nomenclature

α	Angle of attack
A	Area
A_b	Burning area
a	Acceleration
A_e	Exit area
AR	Aspect Ratio
A_{ref}	Frontal area of the missile
A_t	Throat area
b	Web thickness
b_{wing}	Wingspan
c^*	Characteristic velocity
C_{D0}	Zero lift drag coefficient
C_F	Thrust coefficient
C_N	Normal force coefficient
$C_{N,\alpha}$	Normal force coefficient slope
C_0	Overall drag coefficient
d	Diameter
Δt	Timestep
δ_{LE}	Wing's section leading edge angle

Λ	Leading edge sweep angle
dist	Distance
D	Drag
E	Young modulus
ϵ	Static margin
f	Resonance frequency
g_0	Gravitational acceleration at sea level
$\dot{\gamma}$	Turning rate
γ	Specific heat ratio
$H_{formation}$	Entalpy of formation
I_s	Specific impulse
K	Scaling factor
L_B	Body length
L_{CC}	Length of the combustion chamber
L	Length of the missile
L_n	Nose length
M_0	Initial mass
M	Mach number
$\dot{m}_P$	Mass flow rate
M_p	Mass of propellant
M_s	Structural mass
m	Mass
M_{mol}	Molar mass
n_W	Number of wings

n_z	Load factor in the normal direction
P	Pareto percentage
P_{CC}	Combustion chamber pressure
P_e	Pressure at the nozzle exit
q	Dynamic pressure
R	Range
r_b	Burning rate
ρ	Density
R_T	Turn radius
t_{bo}	Burnout time
T_{CC}	Combustion chamber temperature
T_e	Temperature at the nozzle exit
t	Thickness
T	Thrust
t_{MAC}	Maximum thickness of Medium Aerodynamic Chord
v	Velocity
V_f	Volumetric loading factor
V_P	Propellant volume
v_t	Throat velocity
x_{AC}	Position of the aerodynamic center
X_{CG}	Position of the center of gravity
ϵ	Static margin
y	Generic parameter

Contents

List of Figures

List of Tables

Chapter 1

Introduction

The present report has the purpose to illustrate the procedure adopted to improve the performance of an existing air-to-air missile and to discuss the results obtained from the design process.
The customer's demands are to get an improvement by 20% in terms of range and speed, mantaining a comparable maneuverability with respect to the baseline.
In order to meet the requirements, the following steps are followed throughout the conceptual design process:

- Definition of the scenario and analysis of the requirements and specifications.
- Baseline selection and performances estimation.
- Sensitivity analysis and House of Quality implementation.
- Design process, modelling and computations.
- Final missile configuration analysis.

1.1 Background and baseline selection

Air-to-Air missiles are used by aircrafts to intercept and destroy other aircrafts. In order to successfully fulfill the task, they must rely on higher speed and manouverability with respect to the target, and their effectiveness depends on the implemented type of guidance system and warhead. Depending on the range, they are divided in *short range missiles*, in the category "Within Visual Range", and *medium to long range missile*, in the category "Beyond Visual Range".
There are many types of Air-to-Air missiles, each serving the same purpose in different ways. The existing missile selected as baseline is the AIM-7M Sparrow, a widely deployed medium-range supersonic Air-to-Air missile produced by

Raytheon and mostly used by US and NATO forces. The AIM-7 series is primarily adopted to neutralize high performance enemy aircrafts, thanks to a semi-active radar system, high explosive blast fragmentation warhead, featuring high maneuverability and supersonic speed.
The Sparrow is composed by five major sections: radome, radar guidance system, warhead, flight control system and dual-thrust solid propellant rocket motor.

Figure 1.1: 3D rendering of the baseline missile

The missile is controlled by means of four movable delta wings and no thrust vectoring control, stability is provided by four fixed delta fins located in-line with the movable wings. The nose is fairly sharp to improve its aerodynamic efficiency and the missile presents a bottailing to reduce the base drag contribute. Data regarding the motor were difficult to find, as a consequence the composition as well as the shape of the grain have been reconstructed starting from the available data. A Solid Rocket Motor has been chosen as propulsion system, as it is the most widespread solution for air-to-air combat missiles.
The baseline data are briefly reported in the following table:

Table 1.1: Baseline data

Range $[km]$	37.91	Speed $[^{m}/_{s}]$	964.20	Mass $[kg]$	226.8	Load factor	22.7

Chapter 2

Preliminary analysis

2.1 House of Quality

In order to translate the requirements in engineering design parameters, the tool of the House of Quality analysis has been used as a first step.
In the Demanded Quality area, all three design requirements have been considered with the same level of importance, then, taking into account simple models and relations involving the related physical quantities, some engineering factors have been defined and inserted into the Quality Characteristics area, each of them being related to the main requirements considering their relative impact (see Appendix B).
As a result, the main drivers to consider during the preliminary design phase were defined:

- **Specific impulse**: I_s strongly affects both range and speed
- **Propellant mass**: an increase of M_p has beneficial effects on both range and speed. Such kind of modification can affect the missile's center of gravity and static stability.
- **Inert mass**: a reduction of the inert mass increases both range and speed. Controllability and resonance issues has to be taken into account.
- **Drag coefficient**: a decrease of the drag coefficient positively affects range and speed.

2.2 Range and speed prediction model

In order to compute the baseline performances as well as test the outcomes of different design solutions for the required improvements, a MATLAB code for the

estimation of range and velocity values has been written.
The assumptions made to carry out the conceptual design phase are:

- **Constant altitude**: it has been assumed a flight altitude of $11000\,m$ as this is the flight altitude where the military aircrafts equipped with the Sparrow missiles operate. The trajectory has been assumed to be horizontal. It is important to remark that this is not a simplification, as air-to-air missiles are generally employed with an horizontal trajectory.

- **One DOF analysis**: because of the negligible angle of incidence in the horizontal flight, the rigid body analysis with two or more degrees of freedom does not produce any significant advantage with respect to a 1-DOF model [4].

On the basis of the previous assumptions, the model for range and velocity estimation relies on the equilibrium of the forces acting in the direction of the flight velocity.
The total time of operation is splitted into three parts:

1. **Boost phase**: characterized by the highest acceleration.

2. **Sustain phase**: characterized by an almost null acceleration.

3. **Coast phase**: the last flight phase, during which the propellant is completely burnt and the thrust is null.

A different mass flow rate and thrust level is associated to the boost and sustain phases, according to the grain composition and configuration.
There may be different interpretations of range, depending on the mission and considered technology. For this case the range is intended as the distance travelled by the missile from the launch instant untill its velocity is equal to the target, travelling at a certain assumed speed. When its velocity is lower than the target's, the missile is non considere effective anymore.
The axial force balance gives the equation of motion in the longitudinal direction. Integrating the equation, missile's velocity and position are obtained.
The implemented numerical method computes the values of acceleration, velocity and position with respect to the given input data regarding missile's features, flight condition and target velocity.

$$a = (T - D)/m \tag{2.1}$$

$$v = v + a * \Delta t \tag{2.2}$$

$$dist = dist + v * \Delta t \tag{2.3}$$

$$m = m - \dot{m_P} * \Delta t \tag{2.4}$$

The drag, as better explained later in this report, is computed by an additional MATLAB function.
It is worth saying, regarding the range computation, that the Breguet formula has not been considered as it is valid under too compelling assumptions which do not fit well with the considered design conditions.

2.3 Sensitivity analysis

In order to define a design procedure which targets the most influencing parameters with respect to the stated project requirements, a Pareto sensitivity analysis has been made. For such purpose only those parameters which play a role in the definition of the range and velocity have been considered. By varying one parameter at a time and computing numerically the derivative of the cost function with respect to the varying parameter, a numerical method for the Pareto sensitivity analysis can be implemented.
As an example it is reported the procedure used for calculating the impact of a generic parameter y on the total range R:

1. Calculate the range R using the y of the baseline missile.
2. Define two different values of the y with respect to a small variation, using a defined scaling factor K:

$$y_{1,2} = (1 \pm K) * y_{baseline} \tag{2.5}$$

3. Compute the ranges R_2 and R_1 for the two modified values of y.
4. Compute the adimensional Pareto percentages:

$$P_{y,Range} = ((R_2 - R_1)/(y_2 - y_1)) * (y_{baseline}/R) \tag{2.6}$$

   where the partial derivative of the analytical case $\frac{\partial R}{\partial y}$ has been replaced by $\frac{\Delta R}{\Delta y}$.

The same can be done for the maximum speed.
The considered variable parameters are:

- M_0: initial mass of the missile
- $M_{P,Boost}$: propellant mass devoted to the boost phase
- $M_{P,Sustain}$: propellant mass devoted to the sustain phase

- C_D: overall drag coefficient
- $I_{S,Boost}$: specific impulse related to the boost phase
- $I_{S,Sustain}$: specific impulse related to the sustain phase
- $\dot{m}_{P,Boost}$: mass flow rate related to the boost phase
- $\dot{m}_{P,Boost}$: mass flow rate related to the sustain phase

Considering the last two parameters, they have been considered since the thrust T is computed through following the equation:

$$T = \dot{m_P} * g_0 * I_S \tag{2.7}$$

The MATLAB function *pareto* has been used for plotting the results of the analysis. The absolute values for the adimensional Pareto factors have been taken into account. Some parameters may not appear in the plot if their relative impact is one order of magnitude less with respect to the others.

Figure 2.1: Pareto sensitivity analysis for range and maximum speed

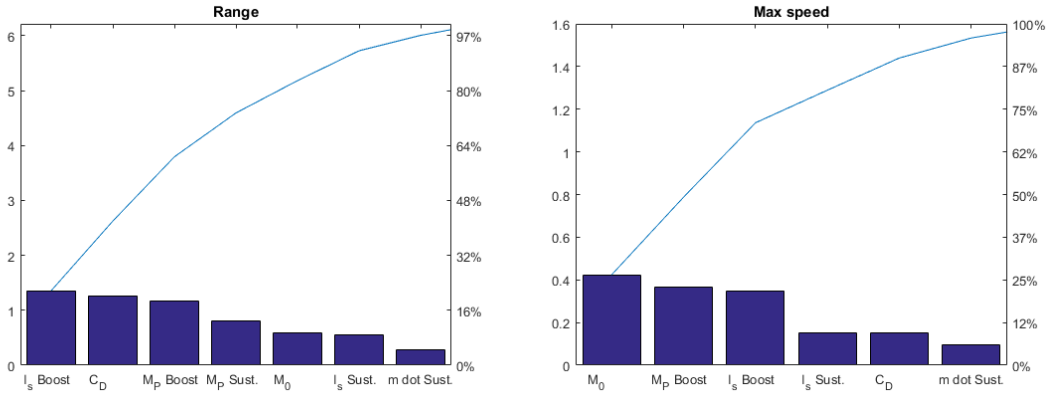

An important consideration emerging from the results is that the main drivers for the range and for the velocity increment do not coincide.
The *80/20 Rule* applied to the Pareto analysis gives the following results, pointing out the parameters which is better to improve in the upgrading process of the baseline missile:

Table 2.1: 80/20 Rule's results

	Increment in range	Increment of max. speed
Decrease of M_0		•
Increase of $M_{P,Boost}$	•	•
Increase of$M_{P,Sustain}$	•	
Decrease ofC_D	•	
Increase of$I_{S,Boost}$	•	•
Increase of$I_{S,Boost}$		
Increase of$\dot{m_{P,Boost}}$		
Increase of$\dot{m_{P,Sustain}}$		

By putting together the results deriving from the House of Quality and from the sensitivity analysis, a methodology of design can be defined. The design procedure has been divided into three main parts:

- **Aerodynamic design**: analysis of the drag sources and reduction of the overall drag coefficient.
- **Propulsive system design**: research of propellant composition and configuration to allow the increase of the specific impulse.
- **Structural analysis and reduction of inert mass**: different approaches to decrease the initial mass will be analysed in order to find the best in terms of acquired performance but without risking to diverge from the initial missile's configuration.

Finally, the results of the three studies are put together in order to fulfill the requirements. A comparison between the selected design solution and the baseline will be made, especially concerning the missile's maneuverability. Some further possible improvements will be analysed.

Chapter 3

Design methodology

In this chapter the parameters selected thanks to the sensitivity analyisis will be considered in order to identify which modifications can be made and can actually improve the baseline design up to the requested values. In particular, three aspect of the missile will be in depth analysed: aerodynamics, propulsion and structure.

3.1 Aerodynamics

The analysis on the aerodynamic part is conducted under the assumption of zero angle of attack $\alpha = 0$. It is important to note that such consideration is merely related to the evaluation of the drag coefficient. During the flight trajectory, α will vary in order to produce the amount of lift required to balance the missile's weight at each instant. However, since in terms of drag coefficient the contribute due to the angle of attack variation does not affect consistently the output value, it has been decided to neglect it. The trajectory is assumed to be horizontal. All aerodynamic surfaces are symmetrical profiles. The following analysis will take into account the four movable surfaces, called *wings*, and the four aft fixed surfaces, called *tail*. The reference theory throughout all the aerodynamic design is the slender body theory, according to which the contributes to the overall C_{D0} to take into account in defining the overall drag coefficient are [4]:

- Base drag
- Friction drag
- Wave drag

All of them are concurring in the body drag coefficient determination, while only wave drag and friction drag are to be considered when evaluating wings and tail contributes.

3.1.1 Body drag analysis

The base drag coefficient refers to the drag generated by the pressure acting on the rear surface of the missile. It is computed by using the following semi-empirical formulas:

Table 3.1: Base drag computation

	Powered phase	Unpowered phase
Supersonic flight	$C_{D0,base} = (1 - A_e/A_{ref}) * \frac{0.25}{M}$	$C_{D0,base} = \frac{0.25}{M}$
Subsonic flight	$C_{D0,base} = (1 - A_e/A_{ref}) * (0.12 + 0.13M^2)$	$C_{D0,base} = 0.12 + 0.13M^2$

Concerning this contribute, the only parameter which can be changed is the base reference area. The other parameters either come from other design phases or are simply given by the flight condition. As shown in the formula, bottailing can be used to reduce the difference between base area and exit area of the nozzle.
A change in the bottail angle from the baseline value of 7.5° to 10° along with a increment of the exit area was made to reduce said drag contribution. The bottail angle chosen is the limit value to avoid flow separation on the external surface of the nozzle.
Concerning the skin friction drag contribute, a simplified approach has been considered assuming:

- Zero-lift flight conditions
- Turbulent flow
- No boat-tail (or negligible, as in the current case)
- No consistent change with altitude of speed of sound and viscosity with respect to the free-stream condition

According to such hypothesis, the following formula for skin friction drag coefficient computation has been implemented:

$$C_{D0,friction} = 0.053 * \frac{L}{d} * (\frac{M}{q * d})^{0.2} \tag{3.1}$$

In order to maintain the cross-section of primary components such as the rocket motor, the guidance system and the warhead, the choice not to change the missile diameter was made. According to this decision, a reduction of the friction contribute can only be achieved by changing the body length. However, since a change in the missile's length affects the stability and the bending frequencies of

the missile itself, it was decided to keep the baseline length value as well, thus to keep the same fineness ratio of the baseline.
The body wave drag is related to the shock waves that occur in supersonic conditions. They are influenced by the nose fineness ratio and bluntness. To reduce such drag contribution a sharp nose is adopted. Concerning the estimation of the body wave drag contribute, the following simplified equation has been used:

$$C_{D0,wave} = (1.586 + \frac{1.834}{M^2}) * [arctan(\frac{0.5}{L_n/d})]^{1.69} \tag{3.2}$$

This semi-empirical formula shows that the higher the nose fineness ratio the lower the wave drag contribution. Due to the previous consideration, any change of the nose fineness ratio has to be achieved thanks to a nose length variation.
Starting from the aforementioned analysis, in order to improve the missile body aerodynamics, the parameters to be changed are the body and nose length. In particular a tradeoff between a body length reduction and a nose elongation is required, maintaining the total missile's length unchanged.
A Matlab function has been implemented in order to reach such a trade-off condition, considering a desired percentage of drag coefficient reduction.
A wave drag reduction of 27% and a skin friction drag reduction of 0.1% have been achieved thanks to a nose elongation of 10.25 centimeters, and a body length reduction of 10.71 centimeters allowing an overall body drag coefficient reduction of 10.17% at Mach 3, 11000 meters of altitude. The nose elongation is accomodated by free space made availible by the guidance and control section reduction, and resulting slight change of 0.46 centimeters over the missile's total length can be assumed as a negligible variation with respect to the baseline value, thus preserving the decision of maintaining the same total length.
A greater reduction would have been possible by a greater nose elongation, but this would have enhance the already existing stress and heat problems, or by a further shortening of the body length, however, it would have certainly caused problems housing all other missile's sections.

3.1.2 Wings and tail analysis

Starting from the baseline estimation of tail and wings drag contributes, the design of the aerodynamic surfaces was carried out maintaining the areas unchanged to roughly mantain maneuverability. The tip chord, leading edge angle and maximum thickness were also left unchanged. Those impositions are meant to avoid possible structural issues compromising the correct operation of the aerodynamic surfaces.The active contributes over the wings and tail drag coefficients are only friction and wave drag [4].

The wave drag coefficient acting on the wings is modelled by the following formula:

$$C_{D0,wing,wave} = n_w * [\frac{2}{\gamma * M_{\Lambda LE}^2}][\frac{(\gamma+1) * M_{\Lambda LE}^2}{2}]^{\frac{\gamma}{\gamma-1}} * [\frac{\gamma+1}{2*\gamma*M_{\Lambda LE}^2-(\gamma-1)}]^{\frac{\gamma}{\gamma-1}} * sin^2(\delta_{LE}) cos(\Lambda_{LE}) * \frac{t_{MAC} * b_{wing}}{A_{ref}} \tag{3.3}$$

Regarding the skin friction drag coefficient, the following semi-empirical formula has been used:

$$C_{D0,wing,friction} = n_w * [0.013 * (\frac{M}{q * L})^{0.2}] * (\frac{2 * A_{wing}}{A_{ref}}) \tag{3.4}$$

The corresponding drag contributes obtained for the baseline missile, at Mach equal to 3 and 11000 meters of altitude, are:

- $C_{D0,wing,wave} = 0.0269$
- $C_{D0,wing,friction} = 0.0958$

for the same flight conditions, the corresponding tail drag coefficient contributes are:

- $C_{D0,tail,wave} = 0.0031$
- $C_{D0,tail,friction} = 0.0588$

A further reduction of the drag coefficient can be achieved by increasing the sweep angle of the aerodynamic surfaces. A Matlab function has been implemented in order to obtain a new sizing of wings and tail simply changing the corresponding sweep angles, but maintaining the same areas. The outcomes, enabling an improvement over the wings and tail drag coefficient contributes, features the modifications reported in Tab. A.1.
Such changes allow the following improvements:

- A decrement of the $C_{D0,wing}$ of 16.54% with respect to the baseline value
- A decrement of the $C_{D0,tail}$ of 10.54% with respect to the baseline value

Again, those results are still referred to the assumed flight condition featuring Mach equal to 3 and an altitude of 11000 meters. As a consequence of the sweep angles changes, also the mean aerodynamic chords were modified resulting in an ulterior decrement in terms of skin friction contribute.

3.2 Propulsion system

Concerning the baseline Solid Rocket Motor only few data were found in the literature due to military secrecy, as a consequence the missing ones were deduced starting from the available. The propulsive system is a dual-thrust (boost+sustain) solid rocket motor and the propellant is known to be an Ammonium Perchlorate and HTPB mixture.

3.2.1 Baseline reconstruction

The available parameters were mostly geometrical data [Tab. A.2] and few ones related to the propellant [Tab A.3] [4].
Starting from fact that only one density information was provided, it was deduced that the grain has a single composition for the two phases. This implies that to obtain the different thrust levels, the burning areas and the grain configurations must be different. Moreover, since the density is quite high for an AP and HTPB mixture, Aluminium particles have to be present too. The following density values have been considered [2]:

Table 3.2: Grain components densities

ρ_{AP} $\left[\mathrm{kg/m^3}\right]$	1950
ρ_{Al} $\left[\mathrm{kg/m^3}\right]$	2700
ρ_{HTPB} $\left[\mathrm{kg/m^3}\right]$	897.183

Thanks to the implementation of a MATLAB function, exploiting a cycle with the densities of the stated ingredients, different weight percentage combinations were computed.
Being i the AP weight fraction (varied between 68 % and 90 %), j the Al weight fraction (varied between 0 % and 20 %) and k the HTPB weight fraction (varied between 10 % and 32 %), the density of the compound is computed as following [9]:

$$\rho_{comp} = \frac{100}{i/\rho_{AP} + j/\rho_{Al} + k/\rho_{HTPB}} \tag{3.5}$$

The nearest composition matching the given density is: AP/Al/HTPB = 73/16/11.
Once the propellant composition is known, together with the information of the nozzle geometry and the combustion chamber pressures, the other parameters can be computed using the *NASA - GLENN Chemical Equilibrium Program CEA*:

- The problem selected is *Rocket*, setting as input data the two different combustion chamber pressures and the area expansion ratio of the supersonic De Laval nozzle.
- The reactants are set according to the previous composition percentages at the reference temperature of 300 K.
- HTPB is added in the user-provided components with the following brute formula [3]:

  $$C_{7.075}H_{10.65}O_{0.223}N_{0.063} \tag{3.6}$$

  with $H_{formation} = -58\,kJ/mol$.

- The simulation is run considering a frozen flow composition with the frozen point placed in the throat section.

The choice concerning the frozen flow composition was made considering a conservative approach, since the frozen flow model is known to underestimate the real performances of about 10%, while the shifting equilibrium overestimates the real performance of about 5%. Concerning the frozen point placement, having no precise information on the dominant reactions during the combustion process, the freezing point is placed by convention in correspondence of the throat section [9]. No other losses are considered, apart from the frozen model underestimation. A simulation was run considering the finite-area combustor but, since the error on the results resulted to be less than 1 % considering the main output parameters, it was decided to keep using the infinite-area combustor.
From the *CEA* output sheet, the considerations were mainly focused on the flow and performance parameters, not considering the thermodynamic quantities and the composition of the exhaust gas. In a more refined analysis these aspects can be further studied and exploited as parameters that may drive performance improvements.
The parameters selected from the analysis and used to complete the baseline data set are in Tab. A.4.
Furthermore, the mass flow rate and the thrust level of each phase were computed as following [9]:

$$\dot{m}_P = P_{CC} * A_t / c^* \tag{3.7}$$

$$T = \dot{m}_P * v_e + (P_e - P_{amb}) * A_e \tag{3.8}$$

The nozzle appears to be underexpanded for all altitudes during the boost phase, while during the sustain phase it is optimized for an altitude between 6000 m and 6100 m.

Figure 3.1: Thrust Profile

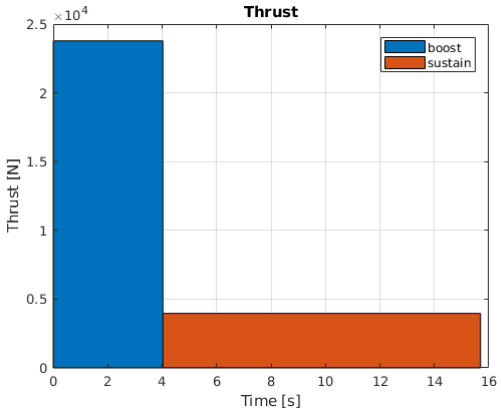

The operating combustion pressures are assumed to be constant during the corresponding phases, which means that also the mass flow rate and the thrust will be considered constant during each phase. As a consequence, under this assumptions, the burn-out time of each phase can be easily computed as the ratio between the propellant mass and the mass flow rate.

$$t_{bo} = M_P/\dot{m}_P \tag{3.9}$$

Table 3.3: Baseline performances

	BOOST	SUSTAIN
Mass flow rate $\dot{m}_P$ [kg/s]	9.9327	1.7138
Total thrust (h = 11 km) T_{tot} $[N]$	23699	3878
Burn-out time $t_{bo}[s]$	4.0271	11.6697

In order to get a more precise estimation, the ignition transient as well as the burn-out phases, along with the combustion instabilities, should be taken into account.
As it was previously considered, the boost phase and the sustain phase do not differ due to their propellant composition but due to the grain configuration. Since the thrust profile necessarily features a neutral burning shape for both phases, the hypothesis of a hollow star grain followed by an end burning grain was the first supposed configuration. However a rapid estimation of the corresponding burning rate lead to discard it:

$$r_b = b/t_{bo} \tag{3.10}$$

Indeed, the resulting burning rate for the end-burning sections would be $r_b = 28.54$ mm/s, not feasible for the considered condition [7].

Figure 3.2: First possible grain configuration

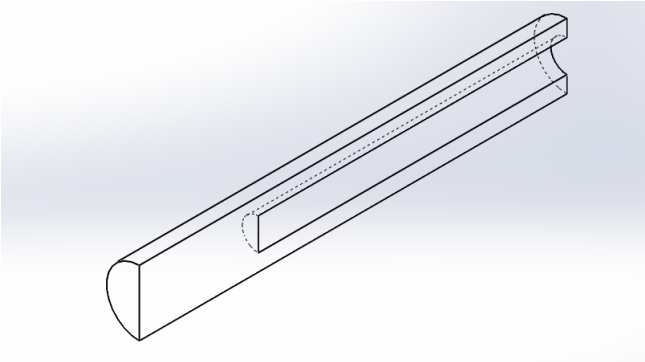

As a consequence, a multi-fin grain configuration was assumed. In order to enable a simplified computation of such complex configuration, the multi-fin geometry was modelled considering two concentric hollow cylinders. The external cylinder for the sustain phase and the internal for the boost phase. The internal diameter of each of the two hollow cylinders is computed starting from the propellant volume of the associated phase:

$$d_{sust} = \sqrt{d_{CC}^2 - \frac{4 * V_{sust}}{\pi * L_{CC}}} \tag{3.11}$$

$$d_{boost} = \sqrt{d_{sust}^2 - \frac{4 * V_{boost}}{\pi * L_{CC}}} \tag{3.12}$$

Taking as reference this simple geometry, the burning rate is estimated considering as web thickness the cylinders' thickness :

Table 3.4: Baseline grain configuration

		Boost	Sustain	
Internal diameter	d_{int}	9.29	17.29	cm
Burning rate	r_b	9.9381	1.2178	$^{mm}/_{s}$

It is worth saying that even though this is a very rough approximation, the resulted values are placed in the feasible range for the considered propellant.
The burning areas needed to reach the required combustion pressures are:

$$A_b = \dot{m_P}/(\rho * r_b) \tag{3.13}$$

According to the assumed simplified geometry, the lateral area is:

$$A_{lat} = \pi * d_{int} * L_{CC} \tag{3.14}$$

Comparing the obtained values of lateral area with the required burning area, it is possible to estimate the actual contribute the fins should give in order to match the two values. The multi-fin profile should give, for the boost phase, a 43 % more lateral surface than a simple hollow cylinder of the same size. Regarding the sustain phase, a 8% more is required.
From the analysis of the rocket motor case geometry: the nozzle occupies $0.13\,m$ over the total length while the ignition mechanism $0.05\,m$. This leaves a length of $1.33\,m$ for the combustion chamber. The corresponding volumetric loading factor is computed as:

$$V_f = V_P/V_{CC} = 0.7872 \tag{3.15}$$

Great effort was put into the reconstruction process of the rocket motor baseline. The baseline was computed with such degree of detail to enable more accuracy during the following design procedure. Moreover, conserving as many features as possible of the baseline enables to exploit the existing technologies, materials and facilities.

3.2.2 Propulsion system upgrade

The two parameters that are improved by the new rocket motor design are the specific impulse and the propellant mass. The first step was to keep the motor geometrically unchanged while a different propellant composition was investigated. The objective was to obtain a specific impulse increase just acting on the chemical properties of the propellant.
Propellant compositions completely different from the baseline grain, such as ADN/GAP/Al or AND/HTPB/Al, have been considered in order to achieve the required improvement.
The problem is modeled considering a frozen equilibrium flow. Under this assumption, the considered alternatives seem to be less performing than the original AP/Al/HTPB. That's because the model is not considering the re-energization of the flow throughout the expansion section that would probably make both ADN/GAP/Al and AND/HTPB/Al more eligible than the current baseline composition [3].
In the following design process the decision to keep the same components of the baseline propellant has been made, achieving the required improvement just changing their fraction percentage.
In order to identify the best solution, the sensitivity of the specific impulse with respect to the variation of the mixture composition has been studied. Such evaluation is performed simulating the rocket behaviour with the *CEA* software keeping the same settings defined for the baseline evaluation.
In Tab A.5 are reported the results, where the baseline composition is reported in bold as a term of comparison.
The obtained results brought to the identification of the best new composition: 82% AP, 4% Al, 14% HTPB. Since the density of the new composition is lower , $\rho = 1691\,kg/m^3$, more volume is needed to store the same amount of propellant. This is a consistent drawback, but due to the relevance of the improvement it is worth looking for a trade-off between other parts of the missile in order to make this change.
Another important improvement can derive from an increment of the expansion ratio, since the baseline nozzle does not exploit the full potential of the flow expansion. The choice is to optimize the nozzle approximately at the known operational altitude, targeting an under-expanded boost phase and an almost optimal sustain

phase condition [6]. The choice of the area ratio takes into account some existent geometrical constraints. The missile has a boat-tail ending section to reduce the base drag. The best option would be to match the exit area with the base area but, due to the risk of causing a separation of the air flow on the lateral surface, it is necessary to keep a boat-tail angle of maximum 10°.
Exploiting the *CEA* software to run simulations with different ε values, the best feasible value is found to be $\varepsilon = 10$. No elongation of the nozzle is considered or needed.
According to all the explained design decisions, the new data for the Solid Rocket Motor are reported in Tab A.6.
As a result:

- The composition change alone can give a 5 % increment on the specific impulse value.
- The geometry of the nozzle alone can give a 5.7 % increment on the specific impulse value.
- Combining the combustion chamber improvement together with the nozzle improvement, the specific impulses increases of the 11%.

Finally, in order to further improve the range and velocity, an increment of the propellant mass has been considered. Thanks to the subsequently described structural changes and improvements, which are better explained in the dedicated chapter, it was possible to add up to $5\,kg$ of propellant to the boost phase. As a consequence, grain configuration and rocket motor case geometry has to be reviewed. The change in the propellant density and the addition of mass bring the volume needed to store the propellant up to $V_P = 0.0384\,kg/m^3$.
If the same combustion chamber is kept, the volumetric loading factor increases up to $V_f = 0.91$, which is a risky value for combustion efficiency [9].
Differently, keeping the same baseline value for the volumetric loading factor, the case would require to be $20\,cm$ longer. Such length cannot be reached without causing too severe penalties on the other missile's components. According to these considerations, a compromise is reached setting $V_f = 0.85$. Such choice requires an additional length of $9.33\,cm$ only, which has been obtained with the reduction of the control system.
Such changes result in a new combustion chamber that is $1.4221\,m$ long.
The new grain geometry is designed using the same simplified model which has been used during the baseline reconstruction, keeping the choice of a multi-fin grain configuration as well.

Table 3.5: New grain geometry

	BOOST	SUSTAIN
Internal diameter d_{int} $[cm]$	7.82	17.3
Burning rate r_b $[^{mm}/_{s}]$	9.94	1.14

The sustain internal diameter remains almost constant with respect to the baseline configuration, showing that the length addition compenses perfectly the volume increase due to the lower density of the new propellant. The boost phase internal diameter is reduced due to the propellant mass addiction.
The mass addition also affects the value of the boost burnout time, raising it of 0.74 seconds.

Figure 3.3: Grain comparison

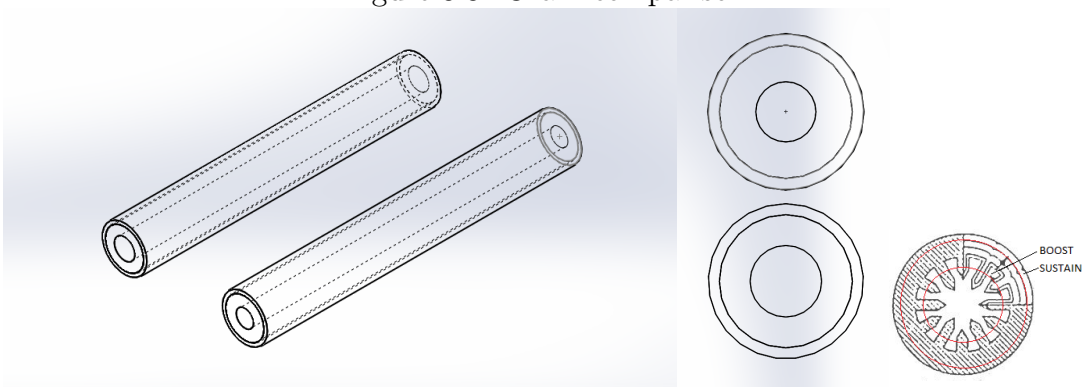

It is worth saying that while the burning rate remains almost constant, the burning area has to increase slightly in order to keep the combustion chamber pressure constant despite the increase of the chamber volume. As a consequence, the multi-fin profile should give, for the boost phase, a 60% more lateral surface than a simple hollow cylinder of the same size. Regarding the sustain phase, a 8% more is required. Compared to the baseline, the boost phase would probably need a higher number of fins in its geometry [8].

3.3 Structure

In order to achieve an additional improvement in terms of range and especially in terms of velocity, a reduction of the inert mass has to be considered. As found in the propulsion system analysis, an additional 5 kg of propellant has to be added in order to achieve these improvements.
The inert mass is mainly composed by the structure and by the control and guidance systems. Both of them will be discussed in the following section, in order to

comprehend if a reduction of one or both of them is feasible and does not upset the baseline design.
For simplicity the missile is divided in six sections, and each of them is assumed to have a mean density which is simply calculated by dividing the mass of each part by its volume, including the structure. The sections are: nose, guidance, warhead, control, motor, nozzle.

3.3.1 Weight reduction

A first reduction of weight has been achieved by reducing the length of the guidance and of the control section to allow the elongation of the nose and of the motor. The reduction of 10 cm of the control section has already been achieved in the development of the AIM-7P version from the AIM-7M, where the hydraulic control system has been replaced with a more volume-efficient one [5]. The reduction of 10 cm of the guidance section can be achieved by asking for a more compact seeker and guidance system, request that can be justified by the evolution in materials since the last modification of the guidance system of the AIM-7M. By doing so, the length of the nose is increased by 10.25 cm to enhance aerodynamic efficiency, and the motor length is increased by 9.33 cm to accommodate the additional fuel. The mass of the nose is kept constant, assuming that the same quantity of material is used and a more refined technological process will be used to achieve the new shape. The burnout mass reduction amount amounts to 9.45 kg, while the reduction of the mass at launch is 4.45 kg.
A second reduction of weight can be achieved by substituting the aluminum of the structure of the guidance and control section with carbon fiber composite material. Such modification can be made following some aerothermodynamic considerations: since the missile flies mainly in supersonic conditions, parts like the nose and the leading edges of the aerodynamic surfaces are subjected to aerodynamic heating, that can interfere with the working condition of the composite. In fact, composite materials can't work at high temperatures (depending on the matrix material, usually 100°C) due to the weaking of the resin matrix and the loss of mechanical properties. If the fluid-thermodynamic field on the missile body does not show peaks of temperature, then the structure can be made of carbon fiber composite, leading to a total reduction in weight of about 12 kg from the baseline, and a reduction of 2.5 kg with respect to the first mass reduction.
A third reduction can be achieved by reducing the thickness of the composite structure to exploit the higher strength of carbon fiber composites. The composite structure has the same thickness of the aluminum one, which is unlikely since composite materials are stronger than aluminum (400 Gpa for high modulus carbonium fiber vs 72 Gpa for aluminum for the Young modulus) and the same structure needs less thickness to withstand the same stresses. Following this basic

structural consideration, the thickness can be reduced from 4 mm from aluminum to 1.5 for composite, with a reduction in weight from variant 2 of about 2.3 kg and a total reduction in weight of about 14.37 kg.
Further weight reductions can be applied to the warhead, motor and nozzle section. A reduction of the warhead would be possible only by changing the whole system with a lighter but more powerful one, since on the warhead destructive capability should remain unaltered. Such new system should have been already tested and approved for flight, thus it would have to be selected from a catalogue. All considered, a brand new warhead design is possible but obviously it is not the best option in this case.
The motor case can also be made out of composite, but it would require a more complex design of the structure and of the insulation/refractory layers, that implies a complex thermodynamic analysis of the motor.

3.3.2 Frequency analysis

A change in the structure leads to a change in the natural resonance frequencies of the missile. Since the missile is actuated to be controlled, a margin must be provided between the frequency of the actuator and those of the structure. A complete dynamic analysis however is too complicate, so a "quick and dirty" method is applied: the missile structure is assumed to be a hollow cylinder with a mean thickness t, a mean modulus E and length L and structural mass M, and the first mode is computed using the following formula:

$$f_1 = \frac{9.87}{2\pi} * \sqrt{\frac{\pi E t}{8 M_s * \frac{L}{d}}} \tag{3.16}$$

The first frequency of the baseline is 43.99 Hz, for version 1 is 44.33 Hz, for version 2 is 58.58 Hz and for the third version is 50.7 Hz.
Assuming that the actuator operates at 16 hz, a safety margin is granted.

Chapter 4

Maneuverability

In order to meet the last requirement an analysis of the various aspects concerning the missile's maneuverability should be done, in order to check whether the new missile's configuration is able to perform according to a comparable level of maneuverability with respect to the baseline.

4.1 Longitudinal static stability

The longitudinal static stability is analysed through the static margin ϵ , that is the difference between the missile center of gravity and the missile aerodynamic center, both divided by the reference missile diameter. This analysis will refer to the worst operating conditions for the studied missile (Mach at launch equal to 2, altitude of 16000 meters). The baseline missile, in these conditions, shows static stability in the considered Mach number range. Indeed, the missile does not require thrust vector control or active control on the movable surfaces. The stable behavior is a feature that needs to be kept for the improved version. Basing the analysis on a model that merges the slender body theory and the cross-flow theory, a semi-empirical formula to calculate the aerodynamic center of the body is provided:

$$\frac{x_{AC}}{L_N} \approx 0.63 * (1 - sen^2(\alpha)) + 0.5 * \frac{L_B}{L_N} * sen^2(\alpha) \tag{4.1}$$

The relation shows that the AC position of the missile body is a property of the nose only. The length of the body has no influence when the angle of attack is low, but it has strong influence when the angle of attack is high. The normal force coefficient slope of the missile body has been calculated by using the following formula:

$$C_{N/\alpha,body} = 2cos(2\alpha)cos(\alpha/2) - ((sin(2\alpha)sin(\alpha/2))/2) + 4(L/D)sin(\alpha)cos(\alpha) \tag{4.2}$$

Basing on the aforementioned assumption of $\alpha \simeq 0$, it is possible to obtain $C_{N/\alpha,body} = 2$.
Regarding the wings and tail aerodynamic centers, the calculation of the normal force coefficients and their slopes are based on two different theories:

- Linear wing theory + Newtonian impact theory: valid for $M^2 > 1 + (\frac{8}{\pi * AR})^2$

$$C_{N,wing} = \left(\frac{4\,|sin(\alpha')cos(\alpha')|}{\sqrt{M^2 - 1}} + 2sin^2(\alpha') \right) * \frac{A_{wing}}{A_{ref}} \tag{4.3}$$

$$C_{N/\alpha,wing} = \frac{4}{\sqrt{M^2 - 1}} * \frac{A_{wing}}{A_{ref}} \tag{4.4}$$

- Slender wing theory + Newtonian impact theory: valid for $M^2 < 1 + (\frac{8}{\pi * AR})^2$

$$C_{N,wing} = \left(\frac{\pi AR}{2} * |sin(\alpha')cos(\alpha')| + 2sin^2(\alpha') \right) * \frac{A_{wing}}{A_{ref}} \tag{4.5}$$

$$C_{N/\alpha,wing} = \frac{\pi AR}{2} * \frac{A_{wing}}{A_{ref}} \tag{4.6}$$

whereα' is the wing effective angle of attack $\alpha^{'} = \alpha + \delta$ and δ is the commanded control angle. Both these theories are valid for $\alpha < 10°$.
The aerodynamic centers of wings and tail, measured from the leading edge of MAC, are dependent on the Mach number, aspect ratio and mean aerodynamic chords:

$$M < 0.7 \Rightarrow x_{AC,wing} = 0.25 * C_{MAC,wing} \tag{4.7}$$

$$M > 2 \Rightarrow x_{AC,wing} = \frac{AR * \sqrt{M^2 - 1} - 0.67}{2AR * \sqrt{M^2 - 1} - 1} * C_{MAC,wing} \tag{4.8}$$

The static margin of the missile is obtained by averaging the contributions of body, wings and tail:

$$\epsilon = -\frac{C_{N/\alpha,body} * (\frac{x_{CG} - x_{AC,body}}{d}) + C_{N/\alpha,wing} * (\frac{x_{CG} - x_{AC,wing}}{d}) + C_{N/\alpha,tail} * (\frac{x_{CG} - x_{AC,tail}}{d})}{C_{N/\alpha,body} + C_{N/\alpha,wing} + C_{N/\alpha,tail}} \tag{4.9}$$

Figure 4.1: x_{AC} and x_{CG} as a function of time

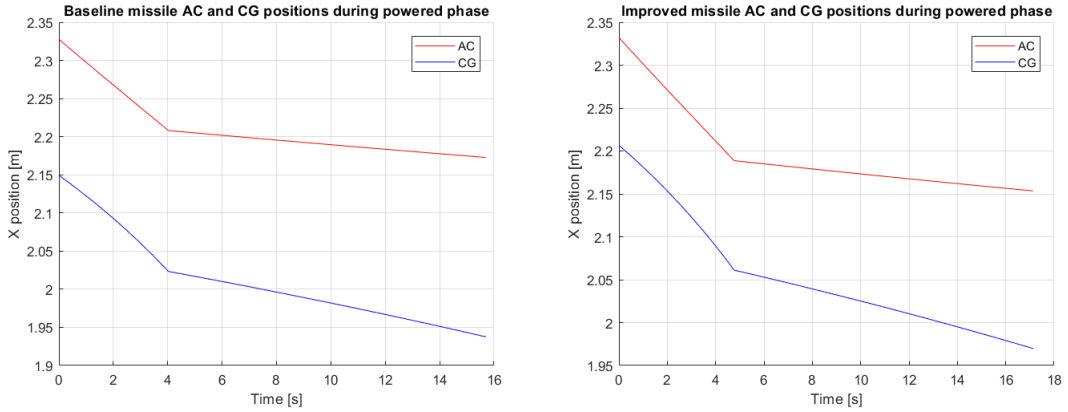

The wings and tail's contribution to the overall aerodynamic center decreases with higher Mach numbers. As the flight speed increases, the aerodynamic center moves towards the nose because the missile body contribution becomes primary. Considering the first version improved missile, the stability has been worsened. As it can be noted in the previous graphs, this result does not come from the aerodynamic center shift but from the center of gravity shift. In the new missile, the x_{CG} at launch is slightly shifted towards the tail due to the increased propellant mass and this affects the stability. At launch (Mach 2, altitude of 16000), the baseline missile's stability values 0.8779, while the improved missile's stability values 0.6178. A higher stability could be achieved by adopting the improved wings and tail which allow their aerodynamic center to shift backward. However, both the versions show stable performances. Finally, the missile maintains its stability through the entire powered flight, from the launch to the burnout. At the end, a last consideration about flares is due: this configuration has not been studied because of its disadvantages in producing higher drag with respect to tail wings, due to incremented front section and in reducing the control capability. However, the flare configuration would have allowed a better stabilization.

Figure 4.2: Static margin as a function of time

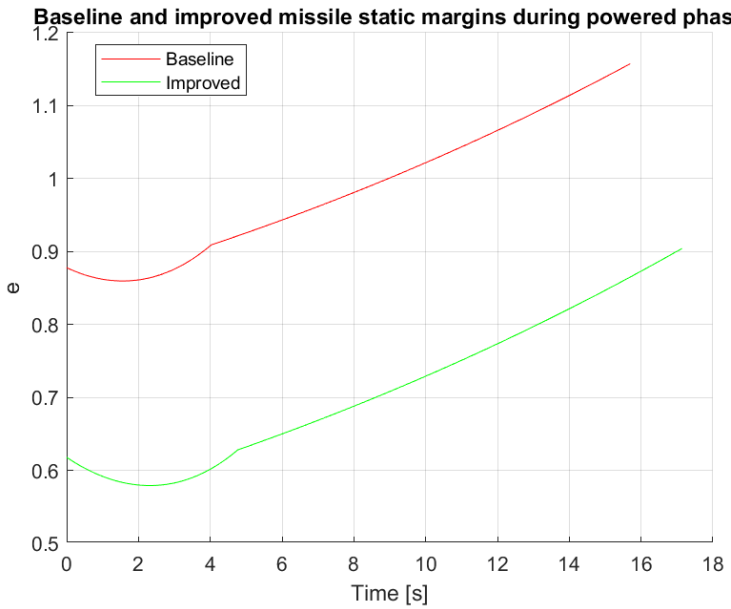

4.2 Turning maneuvers

The turning rate $\dot{\gamma}$ is a parameter that defines the maneuverability of a missile. The rocket must be able to match or surpass the turn rate of the target aircraft in order to successfully intercept it . A second concern in defining the maneuverability is the missile's turn radius R_T that must be less than the turn radius of the target aircraft [4, 1].
A 3-DOF model considering the pitching moment is required for this analysis. Consider the equations of motion for a vertical maneuver turn in the case of winged control:

$$M\dot{\gamma} = \frac{1}{2}A_{ref}\rho V C_N \tag{4.10}$$

The turn radius is calculated as follows:

$$R_T = \frac{2M}{A_{ref}\rho C_N} \tag{4.11}$$

A MATLAB function that evaluates the normal aerodynamic coefficient C_N for the different parts of the missile (body, wings and tail) has been implemented. This function uses the equations coming from the extension of linear wing theory with the Newtonian impact theory. A second MATLAB function is able to calculate

the load factors of each of the three parts of the missile, given the values of C_N, altitude and Mach number:

$$n_{z,body} = \frac{qA_{ref}C_{N,body}}{m_{burnout}g_0} \tag{4.12}$$

$$n_{z,wing} = \frac{qA_{wing}C_{N,wing} * (A_{ref}/A_{wing})}{m_{burnout} * g_0} \tag{4.13}$$

$$n_{z,tail} = \frac{qA_{tail}C_{N,tail} * (A_{ref}/A_{tail})}{m_{burnout}g_0} \tag{4.14}$$

The overall load factor in the normal direction is:

$$n_z = n_{z,body} + n_{z,wing} + n_{z,tail} \tag{4.15}$$

The worst limit condition has been assumed to evaluate the load factor of the redesigned missile:

- Altitude of 16000 m
- Mach = 3 (V = 885 m/s at this altitude)
- The angle of attack of the wing is 22°, a limit value near to the stall condition
- The angle of attack of the body, and as a consequence also of the fixed tail, is 9°

The normal aerodynamic coefficient of the baseline missile has been calculated to be $C_N = 8$. The load factor of the baseline results to be $n_z = 22.7g$. At this point, the computation of the turning performances of the baseline is possible:

$$\dot{\gamma} = \frac{g_0 * n_z}{V} = 0.25 rad/s \tag{4.16}$$

$$R_T = \frac{V}{\dot{\gamma}} = 3540m \tag{4.17}$$

The results obtained from the baseline and the redesigned missile are exactly the same. This can be explained by the simple consideration that in the normal aerodynamic coefficient C_N, which is the parameter that rules the turning performances of the missile, the most important contribution is given by the wings, in particular by their surface. Since in the evolution from the baseline to the modified version of the missile the surfaces of the wings have not been modified, the turning capability remains the same.

Chapter 5

Conclusions

5.1 Final version

At the end of the analysis, what emerges is that the required improvement regarding range and speed cannot be obtained at the same time. The velocity gain, in particular, is harder to achieve and requires more radical changes. In the attempt of getting the best performance improvement at the expense of the minimum change, the final configuration features the following modifications:

- **Structure:**
  - guidance and control system reduction of 20 cm corrisponding to a global reduction of mass of 9.4 kg
- **Aerodynamics:**
  - elongation of the nose of 10.25 cm
- **Propulsion system:**
  - 9.33cm longer motor case
  - new propellant composition AP/AL/HTPB - 82/4/14
  - new nozzle with $\varepsilon = 10$
  - addition of 5kg of propellant to the boost phase

From the sensitivity analysis it can be observed that the Pareto coefficients related to the range weight more than the velocity ones. This means that to get the same improvement of the range on the velocity, the considered parameters have to be heavily modified. Moreover, regarding the velocity, the most influencing parameter is the total mass, which is difficult to reduce without upsetting the baseline too

Table 5.1: Results of the final version

	Range $[km]$	Max. speed $[^{m}/_{s}]$
Baseline	37.91	964.20
Version 1	46.49	1069
Percentual improvement	**22.62%**	**10.90%**

much. On the other hand, the C_{D0} is a parameter that could be improved more easily but it has a positive impact on the range only. With the considered design choices, the range improvement has been evaluated equal to 22.62% , while the maximum velocity is only 10.90% higher with respect to the baseline. The range requirement is abundantly satisfied, while the velocity requirement was too strict to be satisfied without completely transforming the baseline missile.

Figure 5.1: Plots of the final version

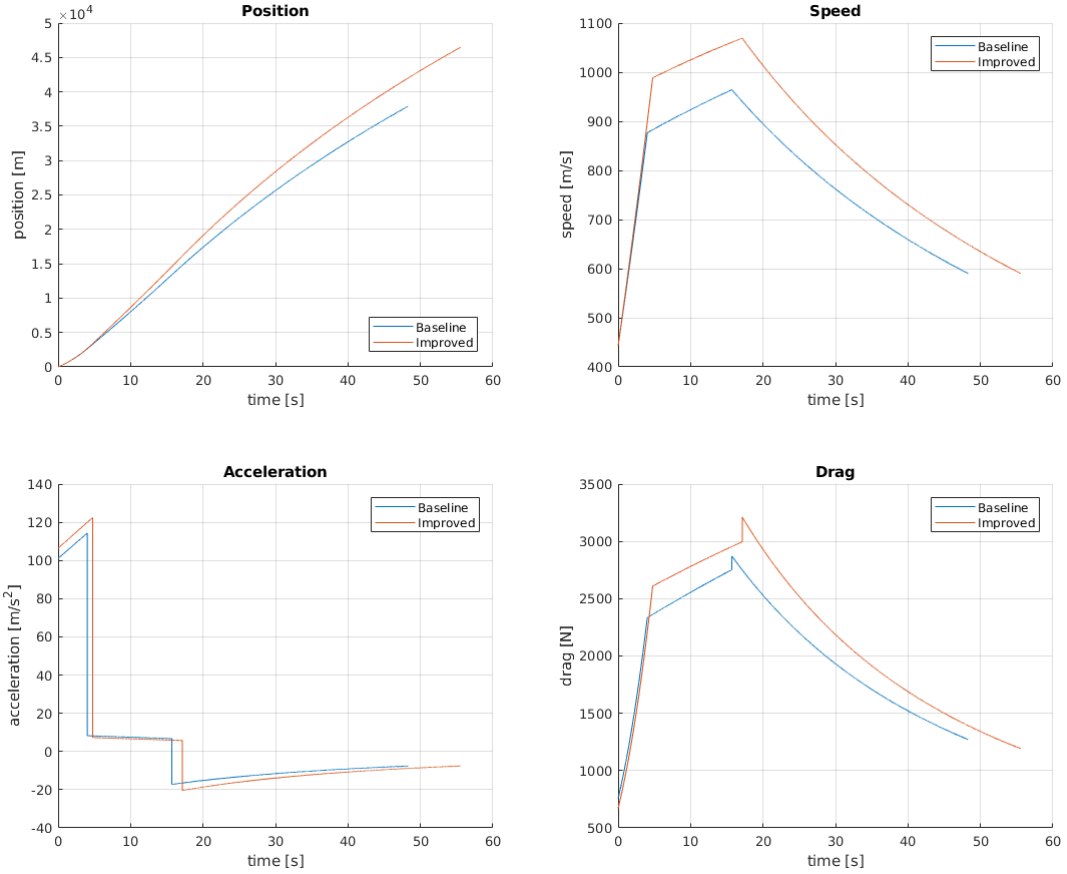

5.2 Further considerations

5.2.1 Less conservative approach

Implementing less conservative improvements, it is possible to match both the requirements. The suggested modifications would include, in addition to the already applied ones:

- **Structure:**
  - composites sections of the structure, resulting in a missile 14.37 kg lighter
- **Aerodynamics:**
  - more efficient wings and stability surfaces
- **Propulsion systems:**
  - enlarged throat section to achieve higher mass flow rate and shorter burning time

  The applied change on the throat section is assumed respecting the limitations on the exit section, which would still be confined inside the reference section area. Keeping the same burn out velocity, the acceleration is achieved in less distance, thus losing less energy due to drag forces. It is worth to stress the fact that the modification implies a severe increase on the mass flow rate. The mass flow rate appears to be a parameter with low influence on the maximum speed, but it is also true that can be widely increased. If increased up to the double, it can strongly affect the performances. The problem with such an increase is that, imposing the combustion pressure constant, the propellant would have to burn much faster, risking to exceed the maximum burning rate value.

Table 5.2: Results of the less conservative version

	Range $[km]$	Max. speed $[^{m}/_{s}]$
Baseline	37.91	964.20
Version 2	45.46	1193
Percentage improvement	**19.91%**	**23.72%**

In this scenario the gains will be of the almost 20% on the range and of about 24% on the velocity, re-equilibrating the performances obtained.

Figure 5.2: Max. speed and Range as function of mass flow rate

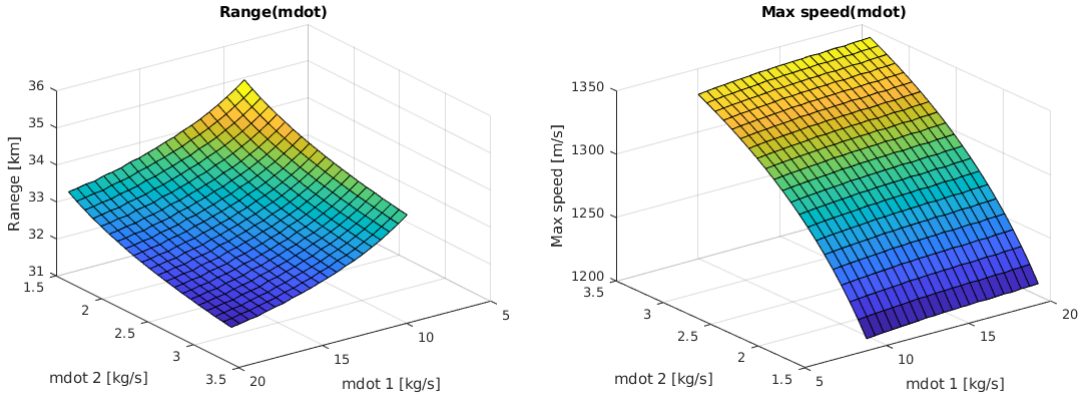

5.2.2 Single phase Solid Rocket Motor

A different approach would feature the use of a single phase Solid Rocket Motor. As can be seen from both the Pareto sensitivity and the plot in Fig. 5.3 taken from the utilized model, the most useful parameter to be varied in order to obtain an increment of the maximum velocity is the mass flow rate of the sustain phase which, if increased, leads to a speed gain. On the other hand an increase in the boost phase's mass flow rate just leads to no significant improvement of the maximum velocity and to a worsening of the range performance. A conceptually easy solution might be to design a single phase rocket motor with the same properties of the boost phase, but with a propellant mass equal to the sum of both boost and sustain phases. This solution can be modelled considering a star grain configuration [8]. As a consequence a big improvement of the maximum speed is obtained, without any loss in terms of range performance.

Table 5.3: Results of the single phase Solid Rocket Motor version

	Range $[km]$	Max. speed $[^{m}/_{s}]$
Baseline	37.91	964.20
Version 3	47.47	1281
Percentage improvement	**25.20%**	**32.81%**

It is worth saying that such good results feature a consistent drawback: even though with this solution the requirements can be easily satisfied, both missile's overall configuration and mission profile are driven very far from the original baseline ones. Not to mention that changing the missile's motor from a two phases to a single phase one could cause many problems that have not even been considered

Figure 5.3: Plots of the further considerations versions

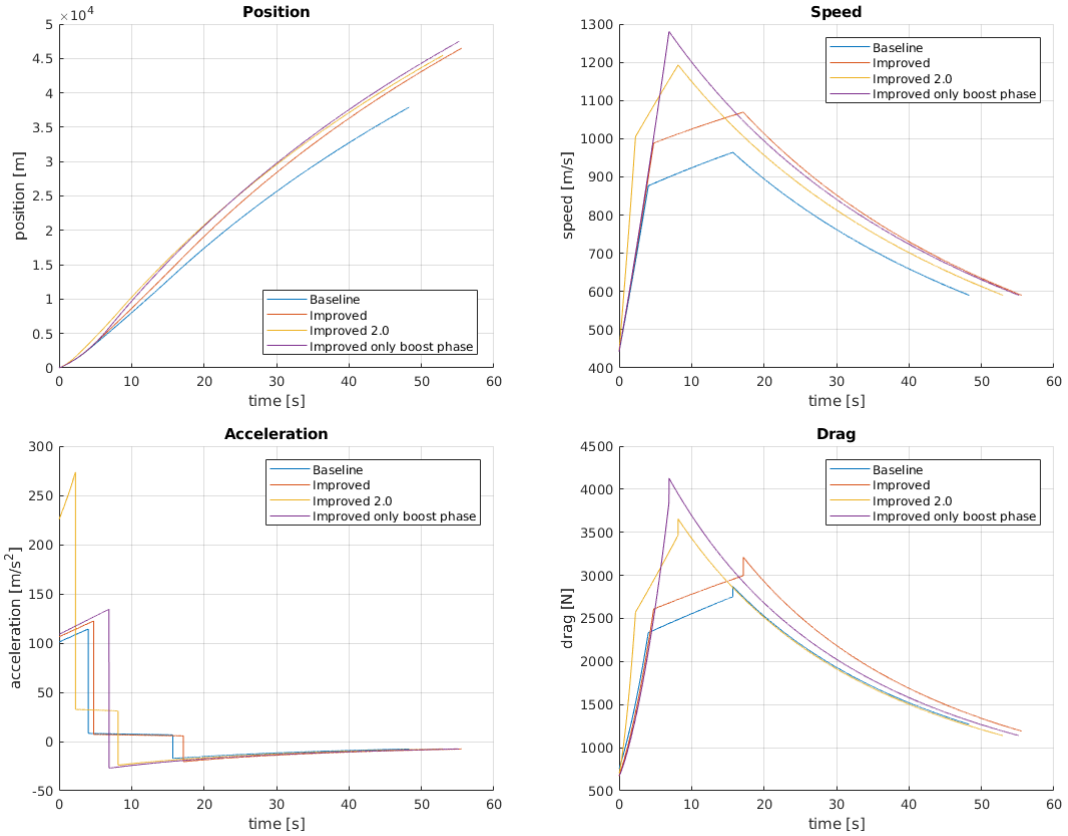

in such a preliminary phase.
In conclusion it is worth remarking that while the 20% increment of the range is a request easily achievable thanks to few modification over the baseline design, the improvement of maximum speed instead requires the design of a completely different rocket.

Appendix A

Tables

Table A.1: Wings and tail comparison

	Baseline	New design
Wing root chord $[m]$	0.4928	0.6731
Wing span $[m]$	0.8179	0.6239
Wing sweep angle	45°	62°
Wing MAC length $[m]$	0.3378	0.4553
Tail root chord $[m]$	0.4699	0.6841
Tail span $[m]$	0.6096	0.4183
Tail sweep angle	57°	73°
Tail MAC length $[m]$	0.3124	0.4561

Table A.2: Solid Rocket Motor: Baseline geometrical data

Rocket Motor Case Length, L_{rmc} $[m]$	1.50876
Combustion Chamber Length, L_{cc} $[m]$	1.3288
Outer Diameter, d_{out} $[m]$	0.2032
Inner Diameter,$[d_{in}]m$	0.20132
Combustion Chamber Area, A_{cc} $[m^2]$	0.0318
Combustion Chamber Volume, V_{cc} $[m^3]$	0.0423
Throat Area, A_t $[m^2]$	0.00116774
Throat diameter, d_t $[m]$	0.0386
Area Ratio A_e/A_t, ε	6.2

Table A.3: Solid Rocket Motor: Baseline propellant data

Density of propellant, ρ [kg/m^3]	1799
Propellant mass total, M_P $[kg]$	60
Propellant mass boost phase, M_{P1} $[kg]$	40
Propellant mass sustain phase, M_{P2} $[kg]$	20
Propellant volume, V_P $[m^3]$	0.0333
Propellant volume boost phase, V_{P1} $[m^3]$	0.0222
Propellant volume sustain phase, $V_{P2}[m^3]$	0.0111
Combustion pressure boost phase, P_{CC1} $[Pa]$	12.2 *10^6
Combustion pressure sustain phase, $M_{CC2}[Pa]$	2.076 * 10^6

Table A.4: Baseline Data from *CEA* analysis

	BOOST	SUSTAIN
Specific Impulse∗g [m/s]	2188.5	2153.8
Specific Impulse, I_S $[s]$	223.1649	219.6265
Characteristic vVelocity, c^* [m/s]	1434.3	1414.5
Throat Flow Density, ρ [kg/m^3]	8.9652	1.5708
Throat Flow Velocity, v_t [m/s]	948.8	934.3
Thrust Coefficient, C_F	1.5259	1.5227
Nozzle Exit Pressure, P_e $[Pa]$	293550	48495
Nozzle Exit Temperature, T_e $[K]$	1751.94	1599.13
Exit Mach Number, M_e	2.918	2.941
Combustion Chamber Temperature, T_{CC} $[K]$	3118.75	2927.83
Throat Flow Molar Mass,M_{mol} [g/mol]	31.108	30.134

Table A.5: *CEA* analysis for Specific Impulse

AP/AL/HTPB	I_SBOOST [m/s]	I_SSUSTAIN [m/s]
73/16/11	**2188.5**	**2153.8**
76/10/14	2241.9	2210.7
78/10/12	2259.8	2226.5
78/8/14	2263.8	2235.4
80/8/12	2281.3	2249.3
82/4/14	2301.6	2280.2

Table A.6: New Solid Rocket Motor performances

	BOOST	SUSTAIN
Specific Impulse $*$g $[^{m}/_{s}]$	2424.6	2401
Specific Impulse in seconds, I_S $[s]$	247.6891	245.2825
Characteristic velocity, c^* $[^{m}/_{s}]$	1507.1	1497
Density of the flow at the throat section, ρ $[^{kg}/_{m^3}]$	8.0036	1.3902
Velocity of the flow at throat section, v_t $[^{m}/_{s}]$	1011.4	997.5
Thrust coefficient, C_F	1.5246	1.5211
Nozzle exit pressure, P_e $[Pa]$	142190	23803
Nozzle exit temperature, T_e $[K]$	1352.78	1296.07
Exit Mach number, M_e	3.331	3.345
Combustion chamber temperature, T_{CC} $[K]$	2980.9	2877.39
Molar mass of the flow evaluated in throat, M_{mol} $[^{g}/_{mol}]$	26.282	26.139
Mass flow rate, $\dot{m}_P$ $[^{kg}/_{s}]$	9.436	1.6169
Total thrust (evaluated at h = 11000 m), T_{tot} $[N]$	24323	3904
Burn-out time, t_{bo} $[s]$	4.769	12.3693

Appendix B

House of Quality

Figure B.1: House of Quality

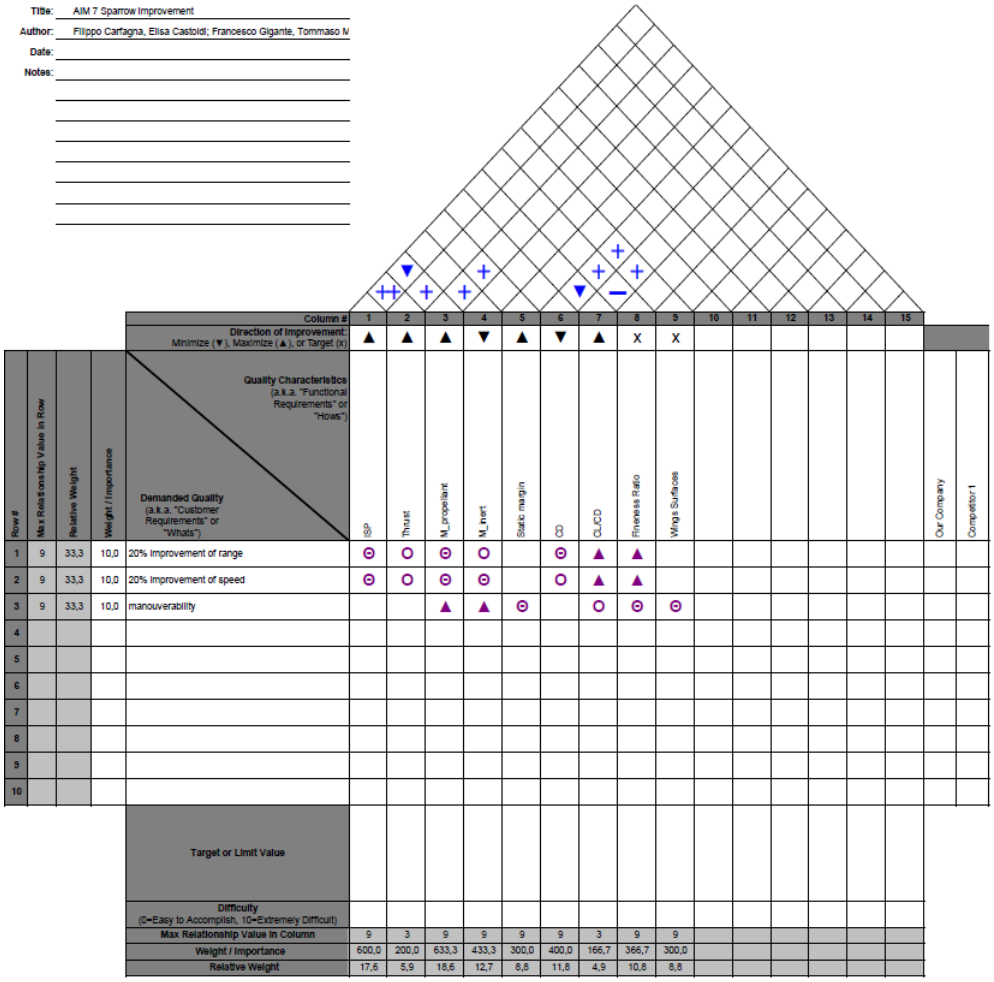

Title: AIM 7 Sparrow Improvement
Author: Filippo Carfagna, Elisa Castoldi, Francesco Gigante, Tommaso M
Date:
Notes:

Row #	Max Relationship Value in Row	Relative Weight	Weight / Importance	Quality Characteristics (a.k.a. "Functional Requirements" or "Hows") / Demanded Quality (a.k.a. "Customer Requirements" or "Whats")	1 ISP	2 Thrust	3 M_propellant	4 M_inert	5 Static margin	6 CD	7 CL/CD	8 Fineness Ratio	9 Wings Surfaces	10	11	12	13	14	15	Our Company	Competitor 1
Column #					1	2	3	4	5	6	7	8	9	10	11	12	13	14	15		
Direction of Improvement: Minimize (▼), Maximize (▲), or Target (x)					▲	▲	▲	▼	▲	▼	▲	x	x								
1	9	33,3	10,0	20% Improvement of range	⊙	○	⊙	○		⊙	▲	▲									
2	9	33,3	10,0	20% Improvement of speed	⊙	○	⊙	⊙		○	▲	▲									
3	9	33,3	10,0	manouverability			▲	▲	⊙		○	⊙	⊙								
4																					
5																					
6																					
7																					
8																					
9																					
10																					
Target or Limit Value																					
Difficulty (0=Easy to Accomplish, 10=Extremely Difficult)																					
Max Relationship Value in Column					9	3	9	9	9	9	3	9	9								
Weight / Importance					600,0	200,0	633,3	433,3	300,0	400,0	166,7	366,7	300,0								
Relative Weight					17,6	5,9	18,6	12,7	8,8	11,8	4,9	10,8	8,8								

Bibliography

[1] S.S. Chin. *Missile Configuration Design*. McGraw-Hill, 1961. pp. 17-53, 107-112,. 4.2

[2] L.T. DeLuca, L. Galfetti, et al. Characterizaton of htpb-based solid fuel formulation: Performance, mechanical properties, and pollution. 2011. 3.2.1

[3] S. Dossi F. Maggi et al. Burning behaviour of adn/an propellants. 3.2.1, 3.2.2

[4] Eugene L. Fleeman. *Tactical missile design, Second Edition*. American Institute of Aeronautics and Astronautics, Inc., 2006. pp. 4-18, 21-78, 197-217, 313-335. 2.2, 3.1, 3.1.2, 3.2.1, 4.2

[5] Forecast international. Aim-7 sparrow. `https://www.forecastinternational.com/archive/disp_pdf.cfm?DACH_RECNO=600`, 2007. 3.3.1

[6] John D. Anderson Jr. *Modern Compressible Flows, with historical perspective, Second Edition*. McGraw-Hill, 1990. pp. 147-163. 3.2.2

[7] Naminosuke Kubota. *Propellants and Explosives*. WILEY-VCH, 2007. pp. 181-183. 3.2.1

[8] Steven D. Stein. Benefits of the star grain configuration for a sounding rocket. 3.2.2, 5.2.2

[9] George P. Sutton and Oscar Biblarz. *Rocket Propulsion Elements*. John Wiley & Sons, 2001. pp. 27-39, 160, 161, 172-189, 417-452, 474-508. 3.2.1, 3.2.1, 3.2.2